Protein Science (1998), 7:413–418. Cambridge University Press. Printed in the USA.

Engineering protein for X-ray crystallography: The murine Major Histocompatibility Complex class II molecule I-A^d

CHRISTOPHER A. SCOTT,[1] K. CHRISTOPHER GARCIA,[1,2] ENRICO A. STURA,[1] PER A. PETERSON,[4] IAN A. WILSON,[1,3] AND LUC TEYTON[2]

[1]Department of Molecular Biology, The Scripps Research Institute, 10550 North Torrey Pines Road, La Jolla, California 92037
[2]Department of Immunology, The Scripps Research Institute, 10550 North Torrey Pines Road, La Jolla, California 92037
[3]Skaggs Institute of Chemical Biology, The Scripps Research Institute, 10550 North Torrey Pines Road, La Jolla, California 92037
[4]R.W. Johnson Pharmaceutical Research Institute, 3535 General Atomic Court, San Diego, California 92121

(RECEIVED July 31, 1997; ACCEPTED October 17, 1997)

Abstract

Class II Major Histocompatibility (MHC) molecules are cell surface heterodimeric glycoproteins that play a central role in the immune response by presenting peptide antigens for surveillance by T cells. Due to the inherent instability of the class II MHC heterodimer, and its dependence on bound peptide for proper assembly, the production of electrophoretically pure samples of class II MHC proteins in complex with specific peptides has been problematic. A soluble form of the murine class II MHC molecule, I-A^d, with a leucine zipper tail added to each chain to enhance dimer assembly and secretion, has been produced in *Drosophila melanogaster* SC2 cells. To facilitate peptide loading, a high affinity ovalbumin peptide was covalently engineered to be attached by a six-residue linker to the amino terminus of the I-$A^d\beta$ chain. This modified I-A^d molecule was purified using preparative IEF and one fraction, after removal of the leucine zipper tails, produced crystals suitable for X-ray crystallographic analysis. The protein engineering and purification methods described here should be of general value for the expression of I-A and other class II MHC–peptide complexes.

Keywords: *Drosophila melanogaster* protein expression; His-tagged protein; preparative IEF; protein deglycosylation; surface plasmon resonance; thrombin digestion; X-ray crystallography

Class II Major Histocompatibility Complex (MHC) molecules are membrane glycoproteins that bind peptide fragments derived from exogenous protein sources, including viral and bacterial pathogens, and transport them to the cell surface for recognition by helper T cells (Cresswell, 1994). Unlike class I MHC molecules, class II MHC molecules are found only on a limited number of cell types (Germain, 1994). These specialized antigen-presenting cells express up to three forms, or isotypes, of class II MHC molecules (Korman et al., 1985; Mengle-Gaw & McDevitt, 1985). Each isotype is encoded at a unique genetic locus. At present, structural information on class II MHC molecules is limited to members of one isotype: HLA-DR in humans, and its murine homologue, I-E. However, the strongest genetic associations of class II MHC molecules with autoimmunity have been established for the other class II isotypes: HLA-DQ and its mouse homologue I-A, and an isotype exclusive to humans called HLA-DP (Lafuse, 1991). In particular, the I-A isotype has been implicated in a number of mouse models of autoimmunity, including diabetes (Wicker et al., 1995), rheumatoid arthritis (Chiocchia et al., 1993), and experimental allergic encephalomyelitis (Martin et al., 1992). It is important, therefore, to investigate whether any unique structural features of I-A molecules can be correlated with autoimmune diseases.

Class II MHC molecules are heterodimeric proteins consisting of noncovalently associated α and β chains. The extracellular portion of each chain consists of one-half of a peptide binding site (the α_1 or β_1 domain) and one Ig-like domain (the α_2 or β_2 domain). Three putative asparagine-linked glycosylation sites, located on the α_1 (α78), α_2 (α119), and β_1 (β19) domains, are present in all class II protein sequences. To date, three different structures of class II MHC molecules have been reported for HLA-DR1 (Brown et al., 1993; Jardetzky et al., 1994; Stern et al., 1994), HLA-DR3 (Ghosh et al., 1995), and I-E^{dk} (Fremont et al., 1996). In these human and mouse class II structures, the amino terminal α_1 and β_1 domains form the characteristic peptide binding groove that was initially described for human (Bjorkman et al., 1987) and mouse (Fremont et al., 1992) MHC class I molecules. The peptide-binding site architecture is formed from two long anti-parallel

Reprint requests to: I. Wilson, Department of Molecular Biology or L. Teyton, Department of Immunology, The Scripps Research Institute, 10550 North Torrey Pines Road, La Jolla, California 92037; e-mail: lteyton@scripps.edu, wilson@scripps.edu.

α-helical segments that sit on top of, and traverse, an eight-stranded anti-parallel β sheet. The peptide-binding domain is supported by the membrane proximal Ig-like domains, and is positioned distal from the membrane surface for interaction with its ligand, the T cell receptor. For most class I and class II MHC molecules, specific positions (or anchors) in the bound peptide are conserved (Rammensee et al., 1995), often corresponding to specific pockets in the peptide binding groove of the MHC molecule that accommodate peptide side chains of a certain size and charge (Saper et al., 1991; Matsumura et al., 1992a). In general, class II MHC molecules will bind peptides that have certain residues located within a nine residue "core" motif. Peptides bound to a class II MHC molecule assume a remarkably regular secondary structure conformation that is similar to a polyproline type II ribbon-like helix (Stern et al., 1994; Fremont et al., 1996; Jardetzky et al., 1996; reviewed in Stern and Wiley, 1994; Wilson, 1996). Importantly, a number of conserved side chains, primarily from the two α-helices, interact with main-chain atoms of the bound peptide and help orient and fix the peptide in the groove (Stern & Wiley, 1994; Jardetzky et al., 1996), imparting a degree of sequence-independent peptide binding capability to the MHC molecule.

X-ray structural studies of I-A molecules require protein in sufficient quantity and quality for crystallization experiments. Soluble I-A^d for crystallization purposes was produced using a leucine zipper to aid in correct heterodimeric pairing of the α- and β-chains (Scott et al., 1996). These I-A^d molecules could then be loaded with specific peptides. However, purification of these I-A^d–peptide complexes by anion exchange chromatography and hydrophobic interaction chromatography did not yield crystals of X-ray diffraction quality. We report here that tethering of a high affinity ovalbumin peptide to the β-chain of the MHC molecule, in conjunction with preparative IEF purification and leucine zipper removal, lead to successful crystallization of an I-A^d–peptide complex that diffracts to 2.6 Å.

Results and discussion

The expression of soluble I-A^d heterodimer using the *Drosophila melanogaster* SC2 cell expression system has been previously reported (Scott et al., 1996). The novel feature of the expression of these recombinant I-A^d molecules was addition of a leucine zipper sequence to the carboxy terminus of each chain to promote subunit dimerization and efficient secretion. Further addition of six histidines to the carboxy terminus of the leucine zipper allowed use of Ni-NTA beads to extract the secreted I-A^d molecules from the SC2 medium. An engineered thrombin-cleavage site was also encoded in the construct prior to the leucine zipper sequence so that the leucine zipper-hexa-histidine tail could be removed later by thrombin digestion.

Drosophila melanogaster cells are not capable of loading peptides onto class II MHC molecules. Newly assembled class II MHC dimers are unstable, and denature in the absence of suitable peptide ligands (Germain & Hendrix, 1991; Sadegh-Nasseri & Germain, 1991). Nevertheless, free exchange of peptides into the MHC binding groove can occur (Bikoff et al., 1993). The peptides most likely come from the growth media itself (Fremont et al., 1995). Indeed, anion exchange of secreted I-A^d did not resolve any discrete fractions, and the profile was consistent with a very heterogeneous population of molecules (data not shown).

Soluble I-A^d was then loaded with a high affinity ovalbumin peptide, $OVA_{323-339}$ (OVA), and purified by anion exchange chromatography. Peptide loading was carried out by mixing a 100:1 stoichiometry of OVA peptide to soluble I-A^d at pH 10.5, followed by neutralization to a final pH of 7.4. Peptide loading could also be achieved using an acidic pH shift to pH 4.5, as previously reported (Lee & Watts, 1990). The I-A^d–OVA complexes are biologically functional, as they activate a T cell hybridoma specific for I-A^d–OVA complexes (Scott et al., 1996). When I-A^d–OVA was analyzed by native IEF, a number of isoforms were visible (Fig. 1, lane 2). Over 400 crystallization screening experiments were performed with peptide-loaded I-A^d, either with the leucine zipper-hexa-histidine tail present or with it removed, but no X-ray diffraction quality crystals could be obtained.

We decided, then, to attempt to reduce the heterogeneity of the MHC-peptide preparations by covalently linking the OVA peptide to the amino terminus of the I-A^d β-chain, as first described by Kappler and co-workers (Kozono et al., 1994; reviewed in Wilson, 1994). We shortened the original 16-residue linker to six residues (GSGSGS) based on the structure of the DR1–HA complex (Stern et al., 1994; PDB accession code 1DLH). Measurement of the distance between the amino terminus of the DR1 β-chain and the carboxy terminus of the HA peptide showed that a six-residue linker would be sufficient to connect the OVA peptide to the I-A^d β-subunit, in order to obtain access to the peptide binding groove. The DNA construct for soluble I-A^d with the covalently bound $OVA_{323-339}$ peptide (I-A^d–cOVA) was then expressed in *Drosophila melanogaster* cells as for soluble I-A^d protein (Scott et al., 1996). Non-reducing SDS-PAGE analysis of Ni-NTA purified I-A^d–cOVA showed three bands with apparent molecular weights of 32, 33, and 35 kDa, and a lower diffuse band corresponding to a

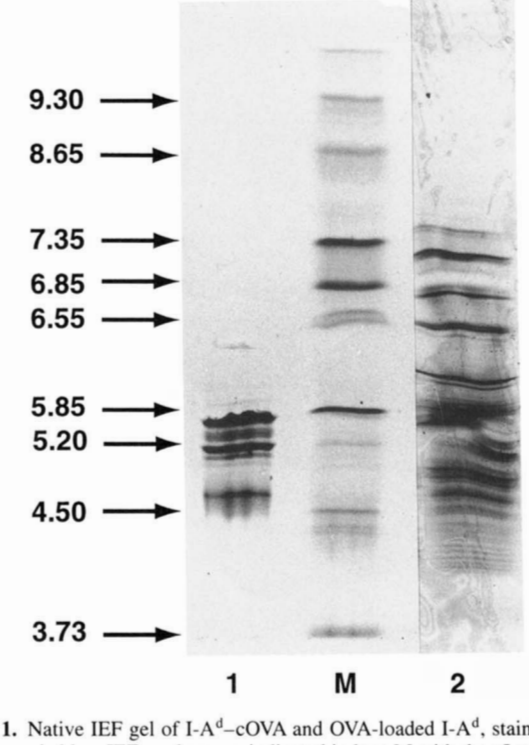

Fig. 1. Native IEF gel of I-A^d–cOVA and OVA-loaded I-A^d, stained with Coomassie blue. IEF markers are indicated in lane M with the pI values on the left side of the gel. Lane 1 shows I-A^d–cOVA. Lane 2 shows I-A^d after loading with OVA peptide. The figure is a composite of two gels, scaled to the same size for comparison.

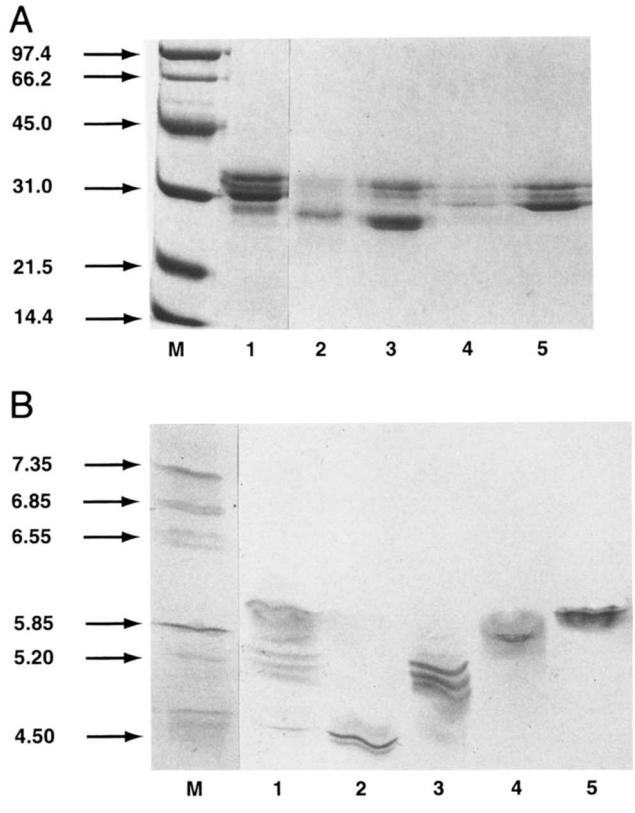

Fig. 2. Analysis of the four fractions that were resolved from the preparative IEF of I-A^d–cOVA. **A**: Nonreducing SDS-PAGE gel (0.1% SDS). Lane 1 is the sample prior to purification. Lanes 2 to 5 correspond to fractions I to IV. The 12.5% acrylamide gel is stained with Coomassie blue. Molecular weight markers (kDa) are shown in lane M. **B**: Native IEF gel, stained with Coomassie blue. Lane 1 shows I-A^d–cOVA prior to preparative IEF purification with reference pI values to the left. Lanes 2 to 5 show preparative IEF fractions I to IV, respectively. IEF markers are indicated in lane M.

molecular weight of 30 kDa (Fig. 2A, lane 1). The three highest molecular weight bands represent different asparagine-linked glycosylation forms of I-A subunits, as endoglycosidase-F/N-glycosidase F digestion shifts the protein mainly to 30 and 31 kDa (data not shown). Native IEF of I-A^d–cOVA revealed a pattern of isoforms with pI values of 4.9, 5.3, 5.4, 5.5, and 6.0, and an indistinct number of isoforms with pI values ranging between 5.6 and 5.9 (Fig. 2B, lane 1). Addition of a covalently linked peptide did not increase the level of protein expression. It did, however, dramatically reduce the IEF heterogeneity of the peptide–MHC complex (Fig. 1, lane 1).

We used surface plasmon resonance to measure direct binding of I-A^d–cOVA to immobilized OVA-2, a soluble T cell receptor (sTCR) specific for $OVA_{323-339}$ bound to I-A^d (Scott et al., 1996). The association rate was derived by fitting the experimental curve by a single association model. The K_{on} was determined to be $2.33 \times 10^4 \pm 1.15 \times 10^4$ M^{-1}/s. The K_{off} could be satisfactorily fit on a single-site dissociation model and was determined to be $2.07 \times 10^{-1} \pm 0.12 \times 10^{-1}$ s^{-1}. The calculated K_d was 8.9 μM, comparable to the calculated K_d of 5.6 μM determined with the $OVA_{323-339}$ peptide-loaded I-A^d (Scott et al., 1996). Control experiments using a sTCR specific for mouse class I MHC K^b in complex with $OVA_{257-264}$ (Carbone & Bevan, 1989), or I-A^d loaded with an influenza peptide $HA_{126-138}$, gave background measurements.

Anion and hydrophobic interaction chromatography failed to produce a fraction of I-A^d–cOVA that readily crystallized. Consequently, we decided to purify I-A^d–cOVA using preparative IEF. An IsoPrime multi-chambered electro-focusing system was used because it does not require addition of ampholytes to the protein sample, and the protein sample has minimal exposure to electrodes. The preparative IEF unit has eight chambers, and can isolate up to eight different protein fractions based on differences in pI. After 12 h of isoelectric focusing, the I-A^d–cOVA sample focused into four of the eight chambers. The four fractions were analyzed by SDS-PAGE (Fig. 2A) and were still heterogeneous in size. Some fractions contained only the 32, 33, and 35 kDa bands (Fig. 2A, lane 5), while other fractions also contained the 30 kDa band (Fig. 2A, lane 3). The differences between fractions were more easily distinguished by non-denaturing native IEF. Chamber three (fraction I) contained an isoform with a pI value of 4.9 (Fig. 2B, lane 2). Chamber four (fraction II) contained three isoforms with pI values of 5.3, 5.4, and 5.5 (Fig. 2B, lane 3). Chamber five (fraction III) contained a smear of isoforms ranging in pI from 5.6 to 5.9 (Fig. 2B, lane 4), and chamber six (fraction IV) contained one isoform with a pI value of 6.0 (Fig. 2B, lane 5).

Each of these four fractions were concentrated and tested for crystallization using 50 published random screen conditions (Jancarik & Kim, 1991), a footprint screen (Stura et al., 1992) and reverse screening (Stura et al., 1994). No conditions for crystallization were found. We next removed the carboxy-terminal leucine zipper-hexa-histidine tail and tested the fractions with the same random screen and footprint screen crystallization conditions. Fractions I to III produced only precipitates, whereas the thrombin-cut fraction IV (Fig. 3A, lane 3) generated crystals in a number of different crystallization conditions. When fraction IV with the leucine zipper tail was analyzed with nonreducing 0.1% SDS-PAGE (without heating to 95 °C) only a small fraction of stable I-A^d dimer was found to be present at 66 kDa (Fig. 3A, lane 1); most of the protein appears to be dissociated α- and β-chains, consistent with previous reports that the I-A heterodimer, in comparison to I-E and HLA-DR heterodimers, are less resistant to SDS-induced denaturation (Germain & Hendrix, 1991; Sadegh-Nasseri & Germain, 1991). The weak association of I-A^d α- and β-chains, and its propensity to aggregate may explain why this isotype has been more difficult to crystallize than the I-E and DR molecules.

After thrombin digestion, the pI of fraction IV shifted to a more acidic pH, giving a tightly clustered set of four different isoforms with pI values of 4.6, 4.7, 4.8, and 4.9 (Fig. 3B, lane 3). Removal of N-linked sugars on I-A^d–cOVA by endoglycosidase F/N-glycosidase F did not change the IEF pattern (data not shown). The source of the IEF heterogeneity remains to be determined, but could be due to multiple conformations, or differences in register, of the bound peptide, as previously suggested (Nag et al., 1994).

The crystal forms produced in the initial crystallization screen by the thrombin-cut fraction IV were spherulites with phosphate as precipitant, "fuzzy balls" with ammonium sulfate, needles with citrate, thin rods with PEG 8000, and diamond-shaped crystals with PEG 600. Crystals grown in PEG 600, 0.1 M imidazole malate, pH 5.5, produced crystals of usable size and morphology for X-ray crystallographic studies. These conditions were derived from the footprint screen (Stura et al., 1992). Washed crystals were analyzed on native IEF gels and consisted primarily of the 4.8 isoform, with some 4.7 and 4.9 isoforms, but lacked the 4.6 isoform (Fig. 3B, lane 5).

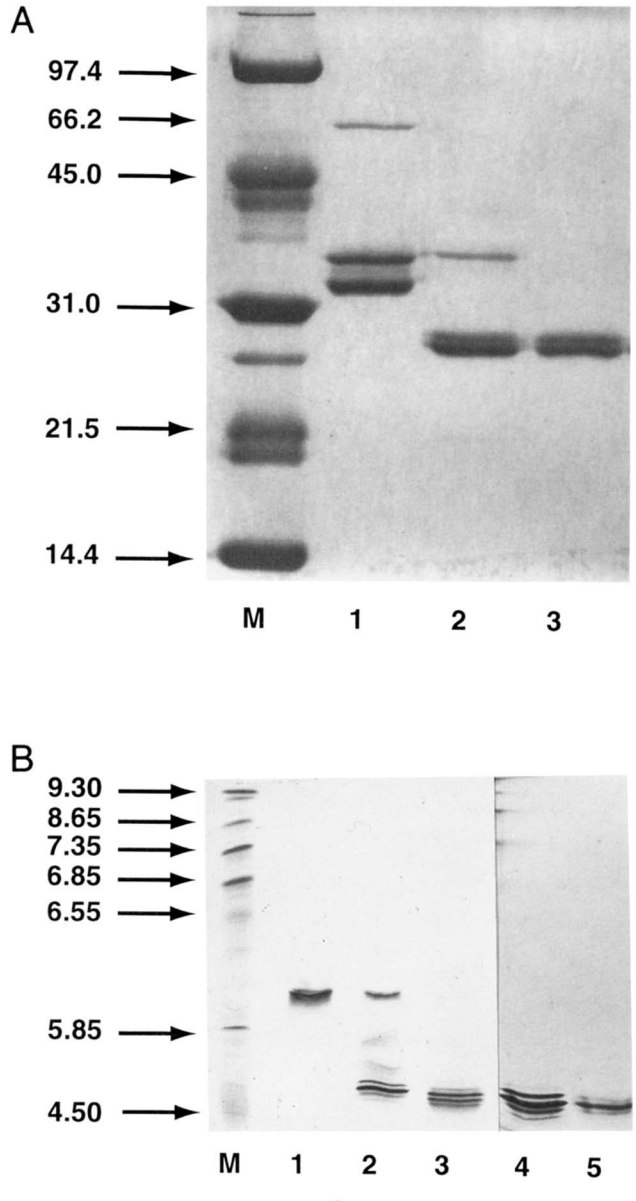

Fig. 3. Analysis of fraction IV of I-A^d–cOVA at various stages of leucine zipper-hexa-histidine tail removal. **A**: Nonreducing SDS-PAGE gel (0.1% SDS) of I-A^d–cOVA before and after thrombin digestion. The 12.5% acrylamide gel is stained with Coomassie blue. Molecular weight markers (kDa) are shown in lane M. Lane 1 shows the sample prior to thrombin digestion. Lane 2 shows the sample after thrombin digestion. Lane 3 shows the thrombin-cut material after a second round of Ni-NTA binding to remove uncut protein. **B**: Native IEF gel, stained with Coomassie blue. IEF markers are indicated in lane M. Lane 1 shows fraction IV prior to thrombin digestion. Lane 2 shows fraction IV after thrombin digestion. Lane 3 shows sample after a second round of Ni-NTA binding. Lane 4 shows the protein sample used to generate the PEG 600 crystals. Lane 5 shows the IEF pattern of a washed and dissolved I-A^d–cOVA crystal grown from PEG 600.

A data set was collected from one crystal at room temperature, and showed diffraction to 3.2 Å resolution. Pseudo-precession analysis of the data using XPREP (Sheldrick, 1994) was consistent with the space group $P4_12_12$ or $P4_32_12$. Indexing of the data with XENGEN (Howard et al., 1987) gave unit cell dimensions of $a = b = 103.7$ Å and $c = 93.3$ Å. The resolution has now been extended to 2.6 Å using a frozen I-A^d–cOVA crystal at the Stanford Synchrotron Radiation Laboratory. The structure determination and refinement of the I-A^d–cOVA complex is underway using these data.

Thus, the experimental approach used for the successful crystallization of I-A^d–cOVA can, therefore, be considered a general method for expressing I-A-peptide complexes and other recalcitrant class II MHC–peptide complexes. The use of preparative IEF demonstrates that separation of specific isoforms of a glycoprotein may be necessary for the growth of X-ray diffraction quality crystals. Indeed, the preparative IEF fraction that produced crystals in PEG 600 also produced crystalline forms in a range of different precipitates, each of which could have been refined and perhaps have lead to alternative ways of producing X-ray diffraction quality crystals.

Materials and methods

Cloning of the I-A^d constructs

Full-length I-A^d α- and β-chains were used as templates for polymerase chain reaction (PCR) amplification of the coding sequence for the extracellular regions of each subunit. For the purpose of cloning, the 5′ primer contained an EcoRI restriction enzyme site, and the 3′ primer contained a Sal I restriction site. In addition, the DNA sequence for an acidic leucine zipper peptide was added to the 3′ end of the truncated I-A^d α gene, and the DNA sequence for a basic leucine zipper was added to the truncated I-A^d β gene sequence (Scott et al., 1996). The 3′ terminus of each insert carried the nucleotide sequence for a hexa-histidine tail. A second version of the I-A^d β-leucine zipper-hexahistidine insert was constructed using PCR amplification to encode the nucleotide sequence of a high affinity 17 mer peptide ($OVA_{323-339}$; ISQAVHAAHAEINE AGR) attached by a six-residue linker (GSGSGS) to the first codon of the mature β-chain. All of these inserts were then cloned into pRMHa3, a previously described vector with a metallothionein-driven promoter (Jackson et al., 1992; Matsumura et al., 1992a, 1992b).

Expression and purification of I-A^d

The pRMHa3 I-A^d α- and β-chain constructs were cotransfected at equimolar ratios with a 1:60 molar ratio of a neomycin resistance gene into *Drosophila melanogaster* SC2 cells using the calcium phosphate precipitation method. Stable cell lines were derived by G-418 selection and kept under selection in Schneider's medium (Gibco BRL, Grand Island, New York) containing 500 μg/mL of G-418 (Gibco BRL, Grand Island, New York). Cell lines were tested for protein expression by a three-day induction of 10 mL confluent cultures with 700 μM copper sulfate. Soluble hexahistidine-tagged I-A^d protein was initially extracted from the SC2 cell culture medium using Ni-NTA beads (Qiagen, Santa Clara, California). Large scale cell culture (18 L) was done in Corning disposable 2-L roller bottles (Corning Costar Corporation, Cambridge, Massachusetts) containing 400 mL of Schneider's medium. Bottles were rotated on a cell-production roller apparatus (Bellco Biotechnology, Vineland, New Jersey), induced for three days, and the media concentrated to approximately 800 mL using a Millipore tangential flow filtration system (Millipore, Bedford, Massachusetts) with a 10 kDa filter.

I-A^d was extracted from concentrated media by antibody affinity chromatography (Scott et al., 1996) using anti-I-A^d antibody MKD6 (Kappler et al., 1981), and in later experiments using Ni-NTA affinity chromatography. In either case, I-A^d was loaded with OVA peptide by eluting the protein with 100 mM diethylamine (pH 10.5) into a solution of phosphate-buffered saline (PBS) and OVA peptide in a 100:1 molar ratio to I-A^d. The mixture of I-A^d and OVA peptide was then immediately neutralized with 2 M glycine. I-A^d–cOVA was extracted from concentrated media using Ni-NTA affinity chromatography. Anion exchange chromatography and hydrophobic interaction chromatography (HIC) of the peptide-loaded I-A^d and I-A^d–cOVA was carried out using an FPLC system (Pharmacia, Alamdea, California). Anion exchange was done using a MONO-Q 10/10 column (Pharmacia, Alameda, California) with a loading solution of 100 mM Tris (pH 7.0), 50 mM NaCl, 0.04% azide, and an elution solution of 100 mM Tris (pH 7.0), 1 M NaCl, 0.04% azide. HIC chromatography was carried out on a Phenyl Superose HR 10/10 column (Pharmacia, Alameda, California) with a loading solution of 50 mM phosphate buffer (pH 7.4), 1 M ammonium sulfate, 0.04% azide, and an elution solution of 50 mM phosphate buffer (pH 7.4), 0.04% azide. All protein concentrations were determined using a BCA protein assay (Pierce, Rockford, Illinois).

Preparative IEF was done using an IsoPrime Multi-chambered Electrofocusing Unit (Hoefer Scientific Instruments, San Francisco, California). The IsoPrime separation module consists of eight separation chambers separated by seven glass fiber filter-reinforced polyacrylamide membranes prepared at the time of purification. The membranes contain covalently incorporated acrylamido buffers that impart to each membrane a unique pK_a value that define steps in a pH gradient. The pI of the affinity-purified I-A^d–cOVA was estimated using analytical IEF run on a PhastGel system (Pharmacia, Alameda, California), and seven pH values (4.5, 4.9, 5.2, 5.6, 5.9, 6.2, and 6.5) surrounding the measured pI of the I-A^d–cOVA were chosen. A software program, Doctor pH (Hoefer Scientific Instruments, San Francisco, California), was used to determine the concentrations of acrylamido buffers needed to make buffer mixtures whose pK_a values matched the selected pH values. Membranes were prepared according to the manufacturer's instructions. The assembled separation module was connected to the IsoPrime circulation system and each chamber filled with a 10% glycerol/water solution. The machine was then run for 2 h to establish the pH gradient within the membranes. After 2 h, the glycerol solution in chamber 2 was replaced with a 30-mL solution of Ni-NTA purified I-A^d–cOVA at a concentration of 0.85 mg/mL, in a 10% glycerol solution; no salts or buffers were present. The IsoPrime was then run at a constant power of 4 watts for 24 h.

Preparative IEF protein fractions were digested with plasminogen-free bovine thrombin (Calbiochem, La Jolla, California) to remove the carboxy-terminal leucine zipper sequence and histidine tag. After a 6-h digestion at room temperature in a 100 mM Tris (pH 7.0), 20 mM NaCl, 0.04% azide solution, the thrombin was inactivated by the addition of AEBSF (4-(2-aminoethyl)-benzenesulfonyl fluoride hydrochloride; Boehringer Mannheim, Indianapolis, Indiana). Ni-NTA beads were added to the sample, and the mixture gently rotated for 1 h to remove any I-A^d–cOVA protein that was not fully digested by thrombin. Finally, inactive thrombin and peptide fragments were removed by anion exchange using a MONO-Q 10/10 column, with a binding solution of 100 mM Tris (pH 8.0), 50 mM NaCl, 0.04% azide, and an elution solution of 100 mM Tris buffer (pH 8.0), 1 M NaCl elution, 0.04% azide. Endoglycosidase F/N-glycosidase F (Boehringer Mannheim, Indianapolis, Indiana) digestion of I-A^d–cOVA was done in a 100 mM phosphate buffer (pH 7.0), 100 mM NaCl, 0.04% azide solution for 3 h at room temperature.

Surface plasmon resonance studies

Measurements were done using a BIAcore 2000 biosensor (Pharmacia, Alameda, California), and data were analyzed using the accompanying BIAevaluation 2.1 software. One thousand response units (RU) of purified OVA-2 sTCR were immobilized to the dextran layer of a CM5 sensor chip by amine coupling. I-A^d–cOVA and peptide-loaded I-A^d were passed through the flow cell at 20 μL/m. The concentration of the MHC–peptide complexes was varied between 1.9 and 30 μM. For control experiments, a second CM5 sensor chip was coated with B3, a sTCR specific for mouse class I MHC K^b in complex with $OVA_{257-264}$ (Carbone & Bevan, 1989).

Crystallization of I-A^d and frozen data collection

All I-A^d and I-A^d–cOVA preparations were initially tested for crystallization behavior using a standard random screen of 50 stock solutions (Jancarik & Kim, 1991) and six reverse screening conditions (Stura et al., 1994). The sitting drop vapor diffusion method was used for all crystallization experiments (Stura & Wilson, 1992). Crystallization experiments were carried out at 22 °C using protein concentrations ranging from 5 to 9 mg/mL. Each sitting drop experiment comprised 2 μL of the protein solution mixed with 2 μL of precipitant solution.

Room temperature data were collected on a Siemens Dual High-Star multiwire area detector mounted on a Siemens generator operating at 40 kV and 55 mA with CuK_α radiation. Frozen data from the I-A^d–cOVA crystals was collected at the Stanford Synchrotron Radiation Laboratories (SSRL) using the in-house open-flow low temperature cryostat to flash cool the crystal to approximately 95 K. In the optimized protocol, a crystal was transferred into a 30% glycerol, 32% PEG 600, 0.1 M imidazole malate (pH 5.5) solution, immediately retrieved in a rayon loop (0.5–0.7 mM diameter; Hampton Research Inc., Irvine, California), mounted, and frozen in the cryostream.

Acknowledgments

We thank Drs. Jeff Speir, Samantha Greasley, Andreas Heine, Massimo Degano, and Brent Segelke for valuable advice and assistance in computational analysis, and Randy Stefanko for assistance in large-scale cell culture and protein production. This work was supported by National Institutes of Health grant CA-58896 (I.A.W.) and R.W. Johnson Pharmaceutical Research Institute (L.T.). This is publication 4-10970-IMM from The Scripps Research Institute.

References

Bikoff EK, Huang LY, Episkopou V, van Meerwijk J, Germain RN, Robertson EJ. 1993. Defective major histocompatibility complex class II assembly, transport, peptide acquisition, and CD4+ T cell selection in mice lacking invariant chain expression. *J Exp Med 177*:1699–1712.

Bjorkman PJ, Saper MA, Samraoui B, Bennett WS, Strominger JL, Wiley DC. 1987. Structure of the human class I histocompatibility antigen, HLA-A2. *Nature 329*:506–512.

Brown JH, Jardetzky TS, Gorga JC, Stern LJ, Urban RG, Strominger JL, Wiley DC. 1993. Three-dimensional structure of the human class II histocompatibility antigen HLA-DR1. *Nature 364*:33–39.

Carbone FR, Bevan MJ. 1989. Induction of ovalbumin-specific cytotoxic T cells by in vivo peptide immunization. *J Exp Med 169*:603–612.

Chiocchia G, Manoury B, Boissier MC, Fournier C. 1993. T cell-targeted immunotherapy in murine collagen-induced arthritis. *Clin Exp Rheumatol 11*:S15–S17.

Cresswell P. 1994. Assembly, transport, and function of MHC class II molecules. *Annu Rev Immunol 12*:259–293.

Fremont DH, Matsumura M, Stura EA, Peterson PA, Wilson IA. 1992. Crystal structures of two viral peptides in complex with murine MHC class I H-2K^b. *Science 257*:919–927.

Fremont DH, Stura, EA, Matsumura M, Peterson, PA, Wilson IA. 1995. Crystal structure of an H-2k^b–ovalbumin peptide complex reveals the interplay of primary and secondary anchor positions in the major histocompatibility complex binding groove. *Proc Natl Acad Sci USA 92*:2479–2483.

Fremont DH, Hendrickson WA, Marrack P, Kappler J. 1996. Structures of an MHC class II molecule with covalently bound single peptides. *Science 272*:1001–1004.

Germain RN. 1994. MHC-dependent antigen processing and peptide presentation: Providing ligands for T-lymphocyte activation. *Cell 76*:287–299.

Germain RN, Hendrix LR. 1991. MHC class II structure, occupancy and surface expression determined by post-endoplasmic reticulum antigen binding. *Nature 353*:134–139.

Ghosh P, Amaya M, Mellins E, Wiley DC. 1995. The structure of an intermediate in class II MHC maturation: CLIP bound to HLA-DR3. *Nature 378*:457–462.

Howard AJ, Gilliland GL, Finzel BC, Poulus TL, Ohlendorf DH, Salemme FR. 1987. The use of an imaging proportional counter in macromolecular crystallography. *J Appl Crystallogr 20*:383–387.

Jackson MR, Song ES, Yang Y, Peterson PA. 1992. Empty and peptide-containing conformers of class I major histocompatibility complex molecules expressed in *Drosophila melanogaster* cells. *Proc Natl Acad Sci USA 89*:12117–12121.

Jancarik J, Kim SH. 1991. Sparse matrix sampling: A screening method for crystallization of proteins. *J Appl Crystallogr 24*:409–411.

Jardetzky TS, Brown JH, Gorga JC, Stern LJ, Urban RG, Chi YI, Stauffacher C, Strominger JL, Wiley DC. 1994. Three-dimensional structure of a human class II histocompatibility molecule complexed with superantigen. *Nature 368*:711–718.

Jardetzky TS, Brown JH, Gorga JC, Stern LJ, Urban RG, Strominger JL, Wiley DC. 1996. Crystallographic analysis of endogenous peptides associated with HLA-DR1 suggests a common, polyproline II-like conformation for bound peptides. *Proc Natl Acad Sci USA 93*:734–738.

Kappler J, Scidmore B, Marrack P. 1981. Antigen-inducible, H-2-restricted, interleukin-2-producing T cell hybridomas. Lack of independent antigen and H-2 recognition. *J Exp Med 153*:1198–1214.

Korman AJ, Boss JM, Spies T, Sorrentino R, Okada K, Strominger JL. 1985. Genetic complexity and expression of human class II histocompatibility antigens. *Immunol Rev 85*:45–86.

Kozono H, White J, Clements J, Marrack P, Kappler J. 1994. Production of soluble MHC class II proteins with covalently bound single peptides. *Nature 369*:151–154.

Lafuse WP. 1991. Molecular biology of murine MHC class II genes. *Crit Rev Immunol 11*:167–194.

Lee JM, Watts TH. 1990. On the dissociation and reassociation of MHC class II-foreign peptide complexes. Evidence that brief transit through an acidic compartment is not sufficient for binding site regeneration. *J Immunol 144*:1829–1834.

Martin R, McFarland HF, McFarlin DE. 1992. Immunological aspects of demyelinating diseases. *Annu Rev Immunol 10*:153–187.

Matsumura M, Fremont DH, Peterson PA, Wilson IA. 1992a. Emerging principles for the recognition of peptide antigens by MHC class I molecules. *Science 257*:927–934.

Matsumura M, Saito Y, Jackson MR, Song ES, Peterson PA. 1992b. In vitro peptide binding to soluble empty class I major histocompatibility complex molecules isolated from transfected *Drosophila melanogaster* cells. *J Biol Chem 267*:23589–23595.

Mengle-Gaw L, McDevitt HO. 1985. Genetics and expression of mouse Ia antigens. *Annu Rev Immunol 3*:367–396.

Nag B, Arimilli S, Koukis B, Rhodes E, Baichwal V, Sharma SD. 1994. Intramolecular charge heterogeneity in purified major histocompatibility class II alpha and beta polypeptide chains. *J Biol Chem 269*:10061–10070.

Rammensee HG, Friede T, Stevanoviic S. 1995. MHC ligands and peptide motifs: First listing. *Immunogenetics 41*:178–228.

Sadegh-Nasseri S, Germain RN. 1991. A role for peptide in determining MHC class II structure. *Nature 353*:167–170.

Saper MA, Bjorkman PJ, Wiley DC. 1991. Refined structure of the human histocompatibility antigen HLA-A2 at 2.6 Å resolution. *J Mol Biol 219*:277–319.

Scott CA, Garcia KC, Carbone FR, Wilson IA, Teyton L. 1996. Role of chain pairing for the production of functional soluble IA major histocompatibility complex class II molecules. *J Exp Med 183*:2087–2095.

Sheldrick GM. 1994. *XPREP—Data preparation and reciprocal space evaluation*. Goettingen, Germany: Siemens Analytical X-ray Instruments.

Stern LJ, Brown JH, Jardetzky TS, Gorga JC, Urban RG, Strominger JL, Wiley DC. 1994. Crystal structure of the human class II MHC protein HLA-DR1 complexed with an influenza virus peptide. *Nature 368*:215–221.

Stern LJ, Wiley DC. 1994. Antigenic peptide binding by class I and class II histocompatibility proteins. *Structure 2*:245-251.

Stura EA, Wilson IA. 1992. Seeding techniques. In: Ducruix A, Giege R, eds. *Crystallization of nucleic acids and proteins*. Oxford, UK: Oxford University Press. pp 99–126.

Stura EA, Nemerow GR, Wilson IA. 1992. Strategies in the crystallization of glycoproteins and protein complexes. *J Cryst Growth 122*:273–285.

Stura EA, Satterthwait AC, Calvo JC, Kaslow DC, Wilson IA. 1994. Reverse screening. *Acta Crystallogr D50*:448–455.

Wicker LS, Todd JA, Peterson LB. 1995. Genetic control of autoimmune diabetes in the NOD mouse. *Annu Rev Immunol 13*:179–200.

Wilson IA. 1994. Covalently-linked ligand stabilizes expression of heterodimeric receptor. *Structure 2*:561–562.

Wilson IA. 1996. Another twist to MHC-peptide recognition. *Science 272*:973–974.